Biochemical and Biophysical Research Communications **274,** 216–224 (2000)
doi:10.1006/bbrc.2000.3054, available online at http://www.idealibrary.com on IDEAL®

Functional Expression and Biophysical Properties of Polymorphic Variants of the Human Gap Junction Protein Connexin37

S. Sindhu Kumari, K. Varadaraj, Virginijus Valiunas, S. V. Ramanan, Emily A. Christensen,* Eric C. Beyer,* and Peter R. Brink

*Department of Physiology and Biophysics, State University of New York at Stony Brook, Stony Brook, New York 11794-8661; and *Department of Pediatrics, University of Chicago, Chicago, Illinois 60637*

Received June 14, 2000

Connexin37 (Cx37) forms gap junction channels between endothelial cells, and two polymorphic Cx37 variants (Cx37-S319 and Cx37-P319) have been identified with a possible link to atherosclerosis. We studied the gap junction channel properties of these hCx37 polymorphs by expression in stably transfected communication-deficient cells (N2A and RIN). We also expressed a third, truncated variant (Cx37-fs254Δ293) and Cx37 constructs containing epitope tags added to their amino or carboxyl termini. All Cx37 constructs were produced by the transfected cells as demonstrated by RT-PCR and immunoblotting and trafficked to appositional surfaces between cells as demonstrated by immunofluorescence microscopy. Dual whole cell patch-clamping studies demonstrated that Cx37-P319, Cx37-S319, and Cx37-fs254Δ293 had large unitary conductances (~300 pS). However, addition of an amino terminal T7 tag (T7-Cx37-fs254Δ293) produced a single channel conductance of 120–145 pS with a 24–30 pS residual state. Moreover, the kinetics of the voltage-dependent decline in junctional current for T7-Cx37-fs254Δ293 were significantly slower than for the wild type, implying a destabilization of the transition state. These data suggest that the amino terminus of Cx37 plays a significant role in gating as well as conductance. The carboxyl terminal tail has lesser influence on unitary conductance and inactivation kinetics. © 2000 Academic Press

Key Words: **intercellular communication; connexin; truncation; frame shift; GFP tag; T7 tag; conductance.**

Gap junction channels facilitate the process of communication between cells in a tissue by directly linking the cytoplasm of two neighboring cells. Gap junction channels can synchronize cellular behaviors through the intercellular passage of cations, anions, metabolites, and second messengers including cAMP, IP_3 and Ca^{2+} (1–4). Gap junction mediated intercellular communication is critical for action potential propagation in electrically excitable tissues (such as the myocardium and smooth muscle), and its importance in coordinating cellular processes between nonexcitable cells (such as in the endothelium) has also been emphasized (5, 6).

Gap junction channels are formed by members of a family of subunit proteins called connexins (Cx). At least 16 different members of this family have been identified and cloned. Functional expression studies have demonstrated that different connexins form channels with differing gating, permeability, and selectivity properties (7). Sequencing and topology predictions have shown that the amino terminus and extracellular and transmembrane regions of these connexins are highly conserved among family members whereas the cytoplasmic domains (a loop in the middle of the molecule and the carboxyl terminus) are unique to each connexin (8). A substantial number of studies have used expression (primarily in *Xenopus* oocytes) of site-directed mutants to correlate sequence features with channel function and regulation. Conclusions from these studies include localization of a number of features to transmembrane and extracellular regions including a voltage sensor (9), pore-forming regions (10), and determinants of docking and heterotypic interactions (11). The carboxyl terminal cytoplasmic domain has been implicated in channel conductance (12) and pH-dependent gating (13, 14).

Several inherited diseases have been associated with mutations in human connexin genes. These connexin-disease associations include: Cx32 with X-linked Charcot-Marie-Tooth disease (15, 16), Cx26 with sensorineuronal deafness (17), Cx46 and Cx50 with cataracts (18, 19) and Cx31 with erythrokeratodermia (20). Most of these mutations are within coding regions and lead to loss of macroscopic intercellular coupling as

0006-291X/00 $35.00

demonstrated in expression systems. A few studies have examined alterations in channel function due to mutations in humans (21). Polymorphic variants of Cx32 (22), and Cx37 (23) and Cx43 (24) have also been reported, but no analyses of functional consequences of these changes have been reported.

We have been studying the biophysical properties of Cx37 channels. Cx37, which is endogenously expressed in endothelial cells and in the developing ovarian follicle, forms gap junction channels that have conductance larger (>300 pS) than any other known connexin (25, 26). A recent report (27) demonstrated that the human population contained two polymorphic variants of Cx37 which differed at position 319 in the carboxyl tail, containing either serine (Cx37-S319) or proline (Cx37-P319); these authors found an association of Cx37-P319 with an increased incidence of atherosclerosis. In the current study, we have examined the channel function of Cx37-S319, Cx37-P319, a (truncated) Cx37 carboxyl tail variant, and an N-terminus tagged form of the truncated Cx37.

METHODS

PCR amplification of human Cx37 cDNA, subcloning and sequencing. Multiple clones of human Cx37 were isolated by hybridization screening of a cDNA library (contained in the bacteriophage vector lambda gt11) prepared from human umbilical vein endothelial cells (25). Cx37-P319 was subcloned into the expression plasmid pSFFV-neo and Neuro2A neuroblastoma (N2A) cells were transfected as previously described (25). Additional clones were constructed by polymerase chain reaction (PCR) amplification (28) from the lambda clones using a sense primer corresponding to the amino terminus with an added *Eco*RI site and a consensus ribosome binding site (29) (5′-GAATTCCACGCCACCATGGGTGACTGGGGCTTC-3′) and an antisense primer corresponding to the carboxyl terminal end with a *Bam*HI site (5′-GACGGATCCACCTATACATACTGCTTCTTAG-AAG-3′). The following antisense primer corresponding to the sequence spanning the frame shift was used to generate Cx37-Δ253; 5′-GACGGATCCACAGTGCCCTGGGTCGGGGGTGC-3′. In some experiments, to subclone into an alternative vector and to incorporate an epitope tag, an alternative antisense primer was used that did not include a termination codon (5′-GACGGATCCACTACATA-CTGCTTCTTAGAAG-3′). *Pfu* DNA polymerase (Stratagene, La Jolla, CA) was used to minimize amplification errors. The PCR products were blunt end ligated into pT7Blue-2 Blunt Vector (Novagen, Inc., Madison, WI). Inserts were fully sequenced (30) using Sequenase 2 (U.S. Biochemical Corp., Cleveland, OH) or using the Big Dye Terminator Cycle Sequencing Ready Reaction Kit and an ABI automated sequencer (Applied Biosystems, Inc., Foster City, CA). For eukaryotic expression, inserts were subcloned into pcDNA3.1 (Invitrogen, Carlsbad, CA). In some cases, to facilitate detection of expression of Cx37 variants, the amplified cDNAs were epitope tagged at the carboxyl terminus by subcloning into the green fluorescent protein vector, pEGFP-N1 (Clontech Laboratories, Inc., S. San Francisco, CA) or the Histidine-tag vector, pcDNA3.1 *Myc*-His (Invitrogen, Carlsbad, CA) or a T7 tag was attached to the N-terminus by PCR.

Cell culture and transfection. Rat insulinoma cells (RIN, ATCC CRL 2058) were obtained from American Type Culture Collection (Manassas, VA) and were grown in RPMI 1640 (GIBCO-BRL) supplemented with 10% heat-inactivated fetal calf serum and, 100 U/ml penicillin and 100 μg/ml streptomycin. Cell cultures were maintained at 37°C and 5% CO_2 in a humidified atmosphere. RIN cells were transfected with linearized plasmids using the calcium phosphate method or the lipofectin (GIBCO-BRL) or effectene reagents (Qiagen, Valencia, CA) following the manufacturer's protocols. Stable neomycin-resistant colonies were selected in 0.1–0.5 mg/ml G418 (Geneticin, GIBCO-BRL).

RT-PCR. Connexin mRNA expression was verified by reverse transcription and polymerase chain reaction (RT-PCR). Total RNAs were extracted from connexin transfected RIN cells using RNA STAT-60 (Tel-Test Inc., Friendswood, TX) following the manufacturer's instructions. RT-PCR reactions were performed using the single tube RT-PCR kit (GIBCO-BRL) and samples were electrophoresed on agarose gels in parallel to molecular weight markers to verify the size and homogeneity of the amplified products.

Detection of proteins directed by plasmid constructs: In vitro translation. The hCx37 constructs in pcDNA-3.1 were transcribed and translated using the TNT quick coupled transcription/translation system (Promega, Madison, WI). The translated proteins were simultaneously labeled using ^{35}S-methionine. The protein samples were electrophoretically resolved on an SDS-containing denaturing polyacrylamide gel, and labeled proteins were detected by autoradiography using Fuji X-ray film.

Immunoblotting. Transfected RIN cells were homogenized in 2× gel electrophoresis sample buffer containing 0.125 M Tris.HCl, pH 6.8, 4% SDS, 10% β-mercaptoethanol, 20% glycerol and 0.004% bromophenol blue (31). Extracts were sonicated for 15 min, boiled for 5 min at 95°C, and clarified by centrifugation; the supernatants were used for experiments. Gel electrophoresis and immunoblotting were performed as described (32). Mouse anti-T7 tag antibody (Novagen, Madison, WI) or rabbit anti-GFP antibody (living colors peptide antibody, Clontech, S. San Francisco, CA) was used for immunoblots.

Immunostaining of transfected cells. Transfected RIN cells grown on sterile coverslips were fixed in freshly prepared ice cold 2% paraformaldehyde/0.1% Triton X-100 in PBS (137 mM NaCl, 2.7 mM KCl, 10 mM $Na_2HPO_4 \cdot 7\ H_2O$, 1.4 mM KH_2PO_4, pH 7.2) for 30 min. Cells were washed twice in cold PBS for 5 min each, blocked with normal goat serum and incubated with primary antibodies at 4°C overnight in a humidified chamber. Primary antibodies included rabbit antibodies raised against the unique C-terminal regions of rat Cx37 (a kind gift from D. L. Paul) and mouse monoclonal antibodies directed against T7-tag (Novagen, Madison, WI) or C-terminal oligohistidine tag (Anti-$(His)_6$ (C-terminal)): Invitrogen, Carlsbad, CA). After washing the slides three times in PBS at room temperature, cells were incubated with FITC-conjugated goat secondary antibodies (Organon Teknika Corporation, Durham, NC) for 45 min. After washing with PBS three times for 5 min, coverslips were mounted using Vectashield mounting medium (Vector Laboratories, Burlingame, CA). Slides were viewed using an epifluorescence microscope with an excitation band filter of 465–495 nm and an emission band pass filter of 515–555 nm and photographed (33).

Confocal microscopy. Transfected RIN cells grown on sterile coverslips were fixed in freshly prepared ice cold 3% paraformaldehyde in PBS for 30 min, washed with PBS (3×) and mounted on slides. Cells were scanned using a 63× oil immersion objective. Confocal microscopy was performed using confocal laser scanning on a Nikon inverted epifluorescent microscope equipped with an argon-krypton laser (Noran Odyssey System, Noran Instruments, Inc., Middleton, WI). Excitation laser lines of 488 nm were used for the detection of FITC labeled antibodies and GFP-tag. Images were collected with a 500 nm band pass filter (green channel). The images collected and stored were analyzed using Meta Morp imaging system (Universal imaging Corp., West Chester, PA). Confocal generated computer images were analysed using Adobe Photoshop 5.0 software (Adobe Systems Inc., Mountain View, CA).

```
Cx37-P319        251 TQGTSSDPYT DQVFFYLPVG QGPSSPPCPT YNGLSSSEQN WANLTTEERL  300

Cx37-S319            .......... .......... .......... .......... ..........  300

Cx37-fs254Δ293        ....PQTLTR TRSSSTS.WA R..HPHHA.P TM.SHPVSRT GPT          293


Cx37-P319        301 ASSRPPLFLD PPPQNGQKPP SRPSSSASKK QYV                     333

Cx37-S319            .......... ........S. .......... ...                     333
```

FIG. 1. Comparison of derived amino acid sequences in the carboxyl terminal regions where Cx37 variants differ. GenBank Accession Nos.: Cx37-P319, M96789; Cx37-S319, AF181620; Cx37-fs254Δ293, AF180815.

Electrophysiological studies. Transfected cell pairs were analyzed by dual whole-cell patch-clamp methods (34–36). Patch electrodes had resistances of 2 MΩ, and were filled with 110 mM CsCl, 1 mM $MgCl_2$, 5 mM EGTA, 0.5 mM $CaCl_2$, and 10 mM HEPES, pH 7.1. The cells were bathed in a solution containing 110 mM CsCl, 1.3 mM KCl, 1 mM $MgCl_2$, 1.8 mM $CaCl_2$, and 10 mM HEPES, pH 7.2. All experiments were performed at room temperature (20–22°C). Transjunctional voltages (V_j) were applied by stepping the holding potential of cell1 (V_1) from a common value ($V_1 = V_2 = 0$ mV, where V_2 is the holding potential of cell2) to a new value in 10 mV increments between −150 and +150 mV. The step sequence was to first apply a prepulse of 10 mV followed by a positive or negative step of a certain amplitude for 400 ms followed by a step of equal amplitude but opposite sign for 400 ms (35). For some experiments the prepulse was 1 s long and the following step protocol employed steps of 10 s. For this latter protocol steps of 5, 10, 15, 20, 25, 30, 50, 70, 90, and 110 mV were employed. Single channel data was collected when activity of only one or two operational channels was observed (6).

RESULTS

Isolation and sequencing of human Cx37 polymorphic variant clones. Because of the recent reports of polymorphic forms of human Cx37 (23, 27), we wanted to isolate cDNA clones for different Cx37 variants and study the channels which they produced in stably transfected cells.

We reexamined the clones which we originally isolated from a human umbilical vein cDNA library (25). We originally isolated more than 10 different phage clones containing Cx37 cDNAs some of which were less than full length (25); the published sequence was a consensus of those sequences. One cDNA clone which was subcloned into pSFFV-neo and expressed in N2A cells was fully sequenced. That sequence (denoted as Cx37-P319) encodes a proline at amino acid position 319 and otherwise matches the sequences published by (27); but contains several differences (likely mistakes due to sequencing errors or consensus formation) from our originally published sequence; a revised sequence has been deposited in GenBank (Accession No. M96789).

We obtained a second clone (Cx37-S319) which is identical to Cx37-P319, except that it encodes a serine at residue 319. Cx37-S319 thus corresponds to the polymorphic variant isolated by others (27).

We also isolated a third variant (Cx37-fs254Δ293). This cDNA is identical to Cx37-S319 except for position 761 (numbered starting from the ATG start codon) where the nucleotide 'C' is absent. This base deletion leads to a shift in the predicted reading frame after 253 amino acids and introduces 40 amino acids of which 34 are different, and a premature TAG stop codon, yielding a predicted polypeptide of 293 amino acids.

These three Cx37 variants all differ within the carboxyl terminal cytoplasmic regions. A comparison of the sequences of these regions is shown in Fig. 1. To further analyze the effects of alterations in the cytoplasmic carboxyl tail of Cx37, we used PCR to create a Cx37 variant that was truncated at approximately the same position as the frame shift (Cx37Δ253). Because available anti-Cx37 antibodies directed against the carboxyl tail of the protein react poorly on immunoblots and would not recognize the truncated Cx37 protein (because of the absence of epitopes), detection of the polymorphic variants was facilitated by preparation of some constructs incorporating T7 epitope tag at the amino terminus or GFP or $(His)_6$ tags at the carboxyl termini. The locations of changes are depicted using topological models of Cx37 in Fig. 2.

We also examined the cDNA sequences and expressed sequence tags (ESTs) which have been deposited in GenBank. Of 19 sequences which span the region encoding amino acid residue 319, nine clones encode proline and 10 clones encode serine, suggesting that as demonstrated by Boerma *et al.* (27), Cx37-P319 and Cx37-S319 are true polymorphic variants. In contrast, none of the deposited sequences contained the Cx37-fs254Δ293 base deletion, suggesting that this may be either a rare polymorphism or a mutation introduced during PCR amplification or cloning. Several sequences encoding either valine or isoleucine at position 130 were also found in the database, suggesting that these may also be true polymorphisms, although only valine was found in any of our clones.

Expression of the Cx37 variants. To examine functional properties of the cell-cell channels produced from the Cx37 variants, RIN cells were stably transfected with polymorphic variants.

Cx37-P319 mRNA expression in N2A transfectants has previously been demonstrated by RNA blotting (25). Expression in RIN cells of Cx37-S319, Cx37-

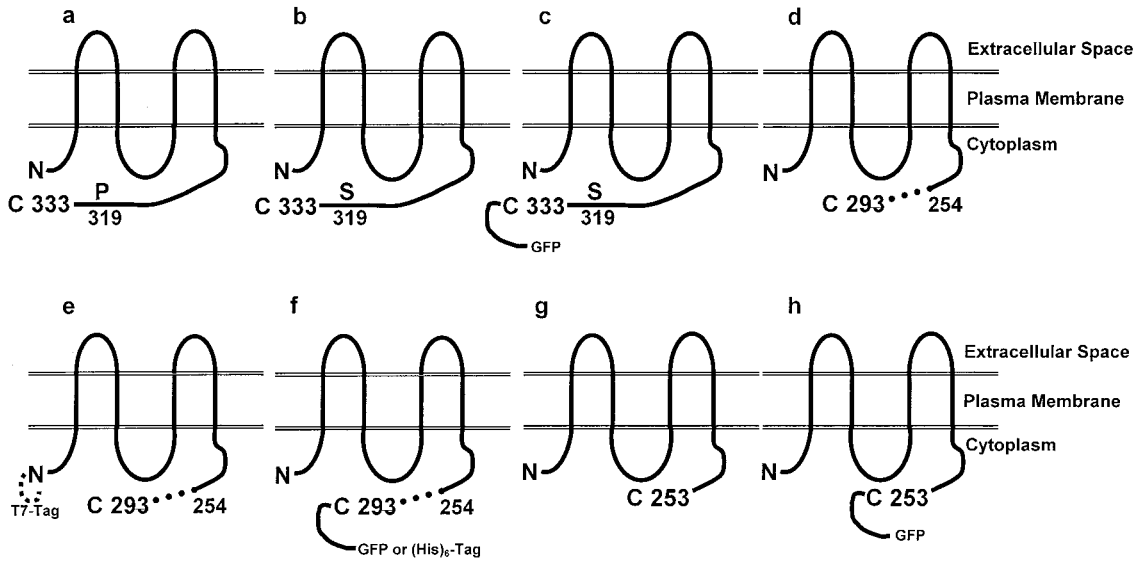

FIG. 2. Topological models of Cx37 variants (a–f) illustrating positions of amino acid differences and nomenclature used throughout this manuscript. All Cx37 variants are denoted as Cx37 with the positions of changes denoted (i.e., substitutions P319, S319; frame shift fs254; and deletions/truncations Δ293, Δ253). In some cases, to facilitate detection of expressed proteins, epitope tags including T7, GFP, and $(His)_6$ were appended to the connexin constructs at the amino or carboxyl ends and are denoted by such an abbreviation preceding or following the connexin mutant name, respectively (e.g., T7-Cx37-fs254Δ293). (a) Cx37-P319; (b) Cx37-S319; (c) Cx37-S319-GFP; (d) Cx37-fs254Δ293; (e) T7-Cx37-fs254Δ293; (f) Cx37-fs254Δ293-GFP or Cx37-fs254Δ293-$(His)_6$; (g) Cx37-Δ253; (h) Cx37-Δ253-GFP.

fs254Δ293 and Cx37-Δ253 mRNAs without and with GFP tag was verified by RT-PCR (Fig. 3a).

We also verified production of the expressed Cx37 proteins. Production of Cx37-P319 protein in N2A cells was previously shown by immunoblotting (35). Examples of *in vitro* translation products and immunoblot detection of Cx37 in the new transfected cells are shown in Fig. 3. *In vitro* translation of Cx37-S319 and Cx37-fs254Δ293 led to production of polypeptides of the expected sizes of 37 and 33 kDa (Fig. 3b, lanes 1 and 2). *In vitro* translation of T7-Cx37-fs254Δ293 and Cx37-S319-GFP led to production of 34 and 64 kDa protein bands, respectively (Fig. 3b, lanes 3 and 4). Immunoblots of RIN cells transfected with Cx37-S319-

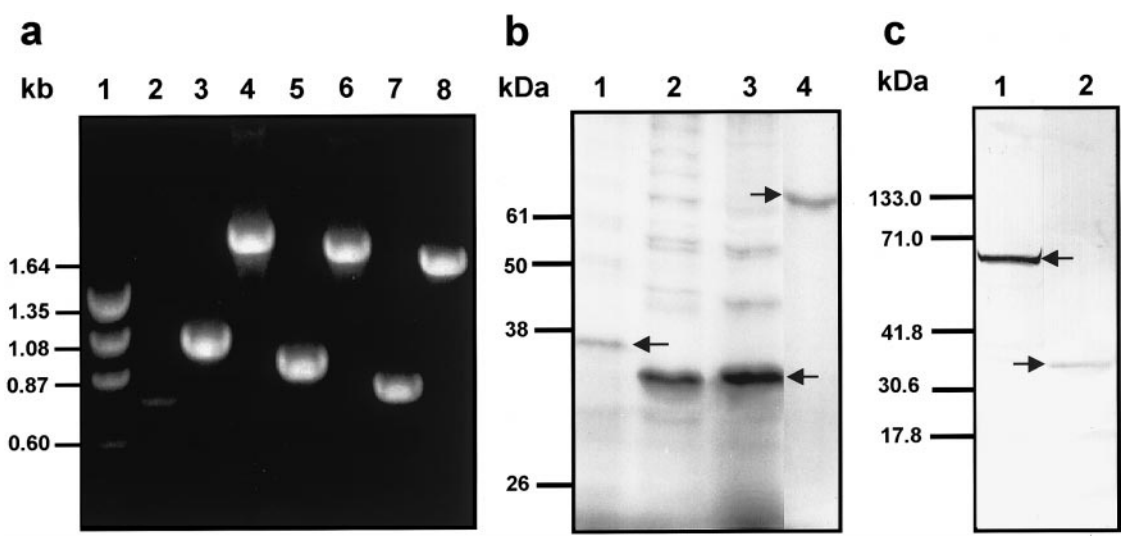

FIG. 3. Verification of Cx37 expression. (a) RT-PCR detection in RIN cells; molecular size marker (lane 1), GFP (lane 2), Cx37-S319 (lane 3), Cx37-S319-GFP (lane 4), Cx37-fs254Δ293 (lane 5), Cx37-fs254Δ293-GFP (lane 6), Cx37-Δ253 (lane 7) and Cx37-Δ253-GFP (lane 8). (b) Autoradiographic detection of *in vitro* translated Cx37-S319 (lane 1), Cx37-fs254Δ293 (lane 2), Ty-Cx37-fs254Δ293 (lane 3), and Cx37-S319-GFP (lane 4). (c) Immunoblot detection of Cx37-S319-GFP (lane 1) and T7-Cx37-fs254Δ293 (lane 2) in lysates of stably transfected RIN cells.

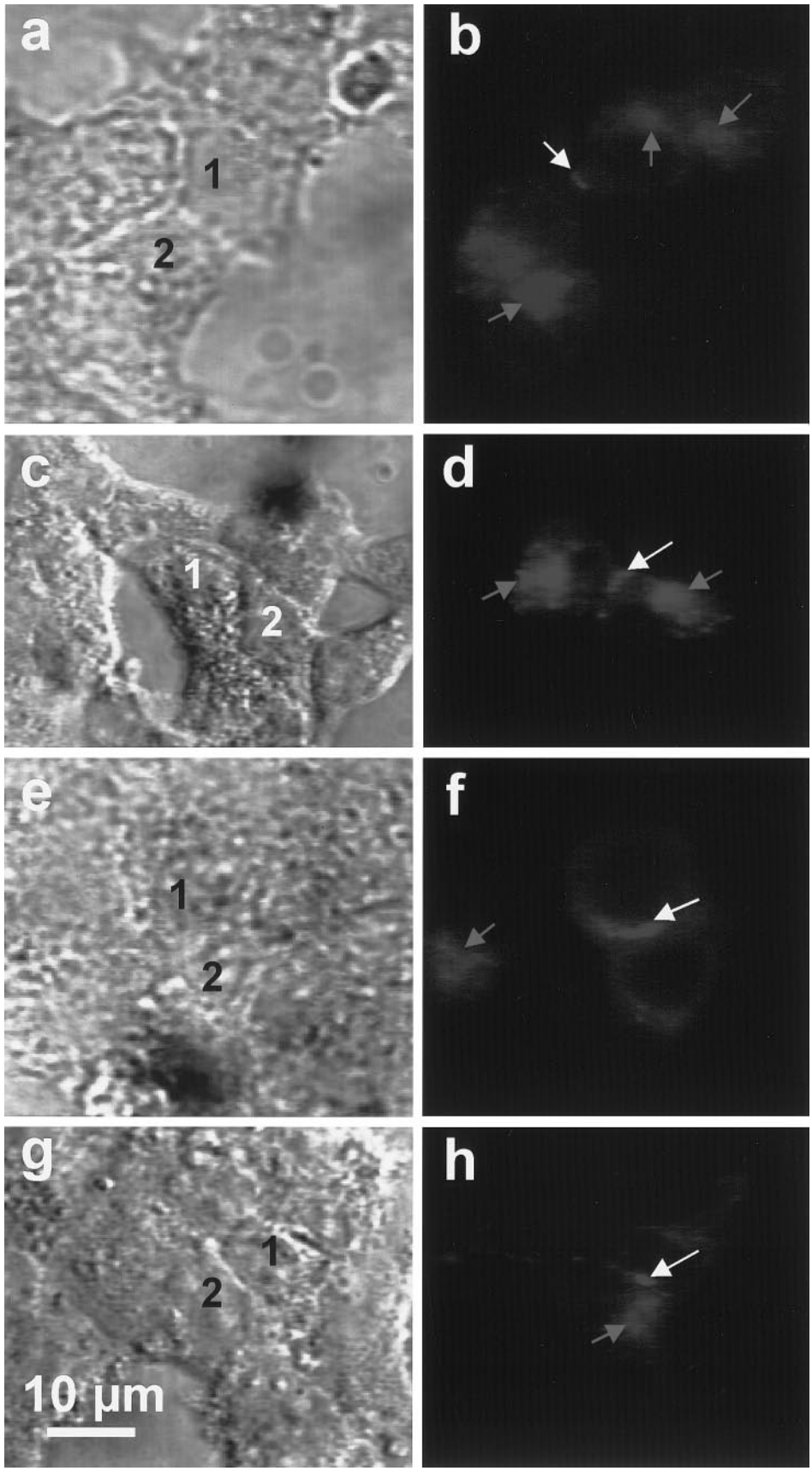
a
1
2
b
c
1
2
d
e
1
2
f
g
1
2
10 µm
h

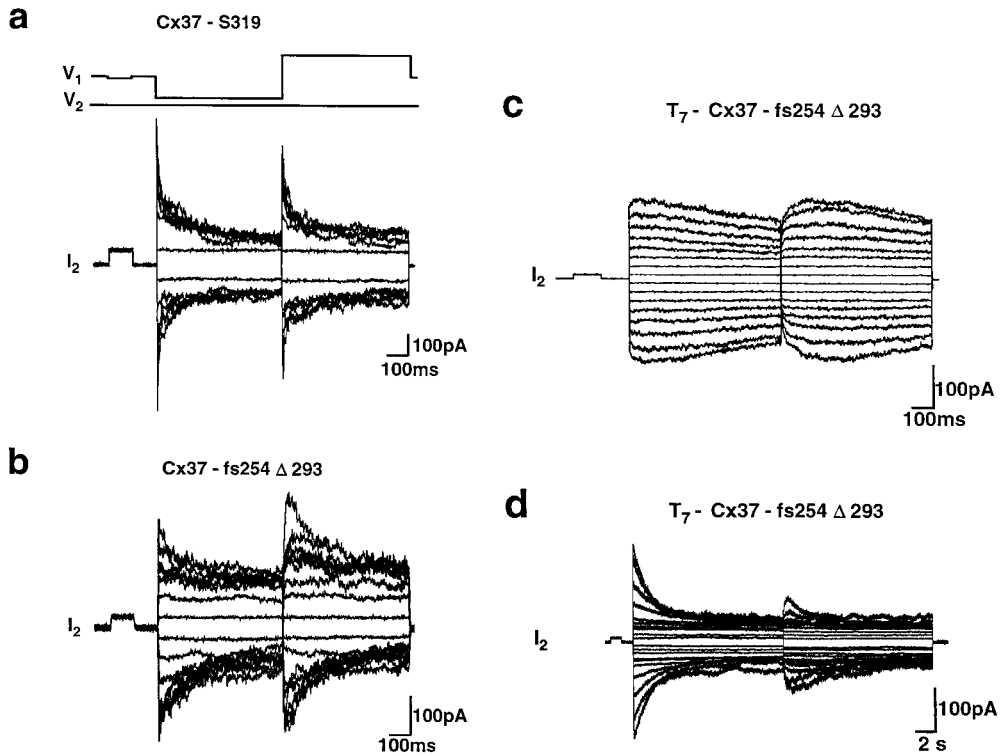

FIG. 5. Macroscopic junctional currents. (a) Cx37-S319: A series of junctional currents are illustrated which result from the application of a step protocol identical to that used by Brink *et al.* (1997) and described under Methods. The duration of the steps was 400 ms. (b) Cx37-fs254Δ293: Same as in (a). (c) T7-Cx37-fs254Δ293: Same as in (a). Note that the kinetics are slowed. (d) T7-Cx37-fs254Δ293: A long voltage protocol of 10 s was used, 5 s. This longer step duration allowed elucidation of the steady state for T7-Cx37-fs254Δ293.

GFP and T7-Cx37-fs254Δ293 (Fig. 3c, lanes 1 and 2) showed major bands that migrated similarly to the expected sizes.

Immunofluorescent staining of cells transfected with unmodified Cx37 constructs or constructs with appended epitope tags all produced similar staining (Fig. 4). All images revealed immunoreactive Cx37 within a diffuse perinuclear cytoplasmic distribution and with a punctate appearance at appositional membranes as expected for gap junctions in the RIN transfectants.

Electrophysiological studies. The properties of channels formed from the Cx37 variants were examined by double whole-cell patch-clamp analysis of stably transfected cells. Examples of the macroscopic junctional currents elicited from cells expressing several Cx37 variants are shown in Fig. 5. Like many other gap junction channels, the Cx37 junctional currents showed a time- and voltage-dependent decay in current magnitude. This voltage-dependent current decay appeared to be relatively similar for all of the carboxyl terminal region alterations (including Cx37-P319 as shown by (25) and Cx37-S319 and Cx37-fs254Δ293 as shown in Figs. 5a and 5b). The only notable difference being a broadening of V_0. In contrast, an alteration of the amino terminal end in T7-Cx37-fs254Δ293 slowed voltage-dependent inactivation dramatically (Fig. 5c), but did not destroy voltage-dependence as shown by application of a long-pulse protocol (Fig. 5d).

Figure 6 shows a comparison of the transjunctional voltage (V_j)-dependence of normalized steady state junctional conductance (G_{ss}) for Cx37-S319 (a, $n = 10$ pairs), for Cx37-fs254Δ293 (b, $n = 6$ pairs) and for T7-Cx37-fs254Δ293 (c, $n = 6$ pairs). Only with pro-

FIG. 4. Detection of Cx37 in stably transfected RIN cells by fluorescence microscopy. (a–h) Confocal laser microscopy with the plane of focus at an intermediate section through the cells expressing Cx37 polymorphs. The arrows indicate either the locations where both contacting cells contribute Cx37 gap junction channels with punctate structures or Cx37 protein localization in the perinuclear region which is characteristic of connexin localization in the Golgi apparatus. (a, c, e, g) Bright field images. (b, d, f, h) Corresponding confocal images. Cells marked 1 and 2 on left are those which show coupling in the corresponding confocal images shown on right. (a, b) RIN cells transfected with Cx37-S319 immunostained with anti-Cx37 antibodies; (c, d) Cells transfected with Ty-Cx37-fs254Δ293 immunostained with anti-T7 tag antibodies; (e, f) Cells transfected with Cx37-fs254Δ293-$(His)_6$ immunostained with anti $(His)_6$ tag antibodies. (g, h). GFP fluorescence in cells transfected with Cx37-fs254Δ293-GFP.

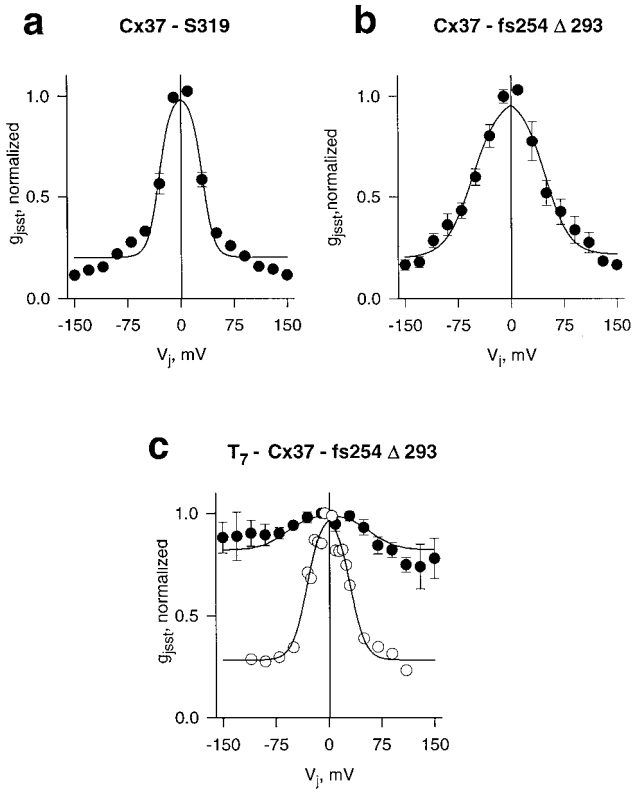

FIG. 6. Normalized steady-state junctional conductance-voltage relationships for (a) Cx37-S319 at the end of 400 ms step, (b) Cx37-fs254Δ293 at the end of a 400 ms step, and (c) T7-Cx37-fs254Δ293 at the end of a 5 s step revealing that the steady state junctional conductance is similar for the wild type and the T7 but that for the latter the time course required is 10–20× greater.

longed voltage steps are the kinetics of voltage inactivation revealed for the T7-Cx37-fs254Δ293 construct. Shorter pulses of 400 ms revealed that the N-terminus tagged Cx37-fs254Δ293 had both activation and inactivation like behaviors for large V_j steps which showed an initial activation or increase in I_j with sufficiently large V_j (±60 mV and greater) followed by a slow decline in I_j. With step durations of sufficient length a steady state was attained which revealed a V_0 of 31 mV which is the same as the Cx37-S319 form (Table 1).

The biophysical properties of all of the carboxyl terminal variants, appeared similar to Cx37-P319 or had slightly reduced unitary conductances relative to Cx37-P319 (3, 25). This includes Cx37-Δ253-GFP, Cx37-Δ253, Cx37-fs254-Δ293. Table 1 shows the difference in the biophysical characteristics of the truncated variant in comparison to Cx37-P319. Since the biophysical properties of Cx37-Δ253 and Cx37-fs254-Δ293 were indistinguishable, data obtained for the two were pooled for Table 1.

Representative single channel records for the full length Cx37 polymorph (Cx37-S319), the truncated Cx37 variant (Cx37-fs254Δ293) and the truncated variant with an amino terminal epitope tag (T7-Cx37-fs254Δ293) are shown in Figs. 7a, 7b, and 7c, respectively. There was no significant difference in the unitary conductance recorded for any of the C-terminal

TABLE 1

Biophysical Characteristics of Cx37 Variants Expressed in Transfected Cells

Cx37 variant	Voltage-dependence, V_0 (mV)	Unitary conductance, γ_j, main state (pS)*-minimum to maximum range
Cx37-P319**	28	300–375
Cx37-S319 (n = 10)	30	348–374
Cx37-fs254Δ293 + Cx37Δ253 (n = 6)	50	277–317
T7-Cx37-fs254Δ293 (n = 6)	31§	60–155

* The range of unitary conductances is shown for each connexin. n, the number of experiments. In all cases CsCl pipette solutions were used.

** Reed *et al.*, 1993; Veenstra *et al.*, 1994; Brink *et al.*, 1997; Ramanan *et al.*, 1999.

§ V_0 determined using the long step protocol.

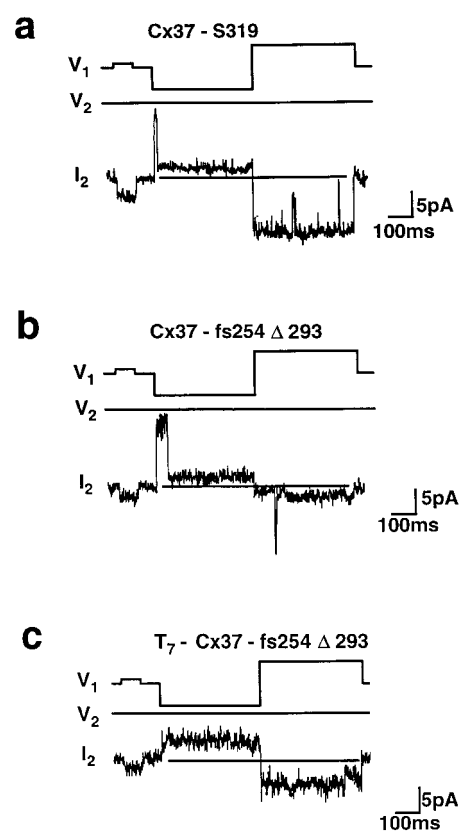

FIG. 7. Single channel records are shown for three cases: Cx37-S319 (a) which shows a main conductance of 370 pS and a subconductance or residual state of 70 pS; Cx37-fs254Δ293 (b) which shows a main state of 330 pS and subconductance state of 100 pS and T7-Cx37-fs254Δ293 (c) which shows a main state of 140 pS. Transjunctional voltage steps of ±30 mV were used in the three cases shown.

variants (data not shown). The range of single channel conductances reported for Cx37, once corrected for salt concentration, is between 300 and 400 pS (26, 37, 38). Furthermore, the residual or subconductance level often observed with Cx37 (26, 37, 38) was present in all cases. In contrast, the amino-terminal tag had a profound effect on unitary conductance. Unitary conductance was reduced by a factor of approximately 2.5–3.0 (7c).

DISCUSSION

Our data show that the unitary conductance and voltage-dependent gating properties of two previously identified polymorphic variants of Cx37, Cx37-P319 and Cx37-S319 (27), are indistinguishable. The properties of a third Cx37 variant (Cx37-fs254Δ293) isolated from the same cDNA library also appears to be similar with only a broadening of V_0. All of the clones did show some passage of Lucifer yellow (data not shown), but the relatively low level of channel expression in these clones made more detailed examinations of permeability/selectivity unrealistic.

Our approach was sensitive to functional changes induced by connexin mutations, since the addition of a T7 tag to the amino terminus of Cx37-fs254Δ293 produced profound changes in both channel gating and unitary conductance. These Cx37 data may not be surprising in view of the series of experiments (39, 40) implicating the amino terminus of Cx32 in voltage-dependent gating. The slowed kinetics but normal steady state (V_o) suggest a destabilization of the transition state between open and closed states. Two explanations are possible. Either the N-terminus tag is physically interacting with the channel orifice or it has caused a conformational change resulting in the apparent destabilization.

Taken together, our data show that the cytoplasmic carboxyl terminal tail of Cx37 has little influence on Cx37 gating and single channel conductance. The data suggest that the C-terminus is not a major contributor to channel gating by transjunctional voltage. With regard to the latter point, our data on Cx37 do contrast with a report which suggested that progressive deletions from the carboxyl terminus of Cx43 altered unitary conductance (12) but are in agreement with other recent observations of unitary conductance made on truncated Cx43 channels (41).

Another point is the broadened V_0 of the C-terminus truncated forms. We have not utilized the longer duration step protocols on these forms to see if they also would conform in terms of V_0 with the Cx37-S319 form with sufficient time to achieve steady state.

Our data suggest that the polymorphic variants detected by Boerma *et al.* (27) might have little influence on a number of properties of Cx37-mediated intercellular communication. One interpretation might be that these are actually silent polymorphisms which only represent disease-associated genetic markers. Alternatively, the carboxyl terminus of Cx37 may be involved in other aspects of the regulation of gap junction-mediated intercellular communication. In Cx43, the carboxyl tail has been implicated in channel gating via three mechanisms. They are: (a) changes in intercellular pH (13, 14), (b) activation of protein kinase cascades (42, 43), and (c) altered dwell time (41). Perhaps future investigations of such "chemical and voltage gating" in mutant Cx37 channels would be appropriate.

ACKNOWLEDGMENTS

This work was supported by grants from the National Institutes of Health (GM 55263 to P. R. Brink; HL 45466 and HL 59199 to E. C. Beyer) and The Bernice Meltzer Pediatric Cancer Research Funds.

REFERENCES

1. Saez, J. C., Connor, J. A., Spray, D. C., and Bennett, M. V. L. (1989) Hepatocyte gap junctions are permeable to the second messenger, inositol 1,4,5-triphosphate, and to calcium ions. *Proc. Natl. Acad. Sci. USA* **86,** 2708–2712.
2. Tsien, R. W., and Weingart, R. (1976) Inotropic effect of cyclic AMP in calf ventricular muscle studied by a cut end method. *J. Physiol. (Lond.)* **260,** 117–141.
3. Veenstra, R. D., Wang, H. Z., Beblo, D. A., Chilton, M. G., Harris, A. L., Beyer, E. C., and Brink, P. R. (1995) Selectivity of connexin-specific gap junctions does not correlate with channel conductance. *Circ. Res.* **77,** 1156–1165.
4. Brink, P. R. (1998) Gap junctions in vascular smooth muscle. *Acta. Physiol. Scand.* **164,** 349–356.
5. Segal, S. S., and Duling, B. R. (1986) Flow controls among microvessels coordinated by intercellular conduction. *Science* **234,** 868–870.
6. Christ, G. J., and Brink, P. R. (1999) Analysis of the presence and physiological relevance of subconducting states of connexin43-derived gap junction channels in cultured human corporal vascular smooth muscle cells. *Circ. Res.* **84,** 797–803.
7. Bruzzone, R., White, T. W., and Paul, D. L. (1996) Connections with connexins: The molecular basis of direct intercellular signaling. *Eur. J. Biochem.* **238,** 1–27.
8. Beyer, E. C., Paul, D. L., and Goodenough, D. A. (1990) Connexin family of gap junction proteins. *J. Membr. Biol.* **116,** 187–194.
9. Trexler, E. B., Bennett, M. V. L., Bargiello, T. A., Verselis, V. K. (1996) Voltage gating and permeation in a gap junction hemichannel. *Proc. Nat. Acad. Sci. USA* **93,** 5836–5841.
10. Zhou, X. W., Pfahnl, A., Werner, R., Hudder, A., Llanes, A., Leubke, A., and Dahl, G. (1997) Identification of a pore lining segment in gap junction hemichannels. *Biophys. J.* **72,** 1946–1953.
11. White, T. W., Bruzzone, R., Wolfram, S., Paul, D. L., and Goodenough, D. A. (1994) Selective interactions among the multiple connexin proteins expressed in the vertebrate lens: The second extracellular loop is a determinant of compatibility between connexins. *J. Cell Biol.* **125,** 879–892.
12. Fishman, G. I., Moreno, A. P., Moreno, D. C., and Leinwand, L. A. (1991) Functional analysis of human cardiac gap junction channel mutants. *Proc. Natl. Acad. Sci. USA* **88,** 3523–3529.
13. Ek-Vitorin, J. F., Calero, G., Morley, G. E., Coombs, W., Taffet, S. M., and Delmar, M. (1996) pH regulation of connexin43:

Molecular analysis of the gating particle. *Biophys. J.* **71,** 1273–1284.

14. Morley, G. E., Ek-Vitorin, J. F., Taffet, S. M., and Delmar, M. (1997) Structure of connexin43 and its regulation by pHi. *J. Cardiovascular Electrophysiology* **8,** 939–951.
15. Bergoffen, J., Scherer, S. S., Wang, S., Scott, M. O., Bone, L. J., Paul, D. L., Chen, M., Lensch, W., Chance, P. F., and Fischbeck, K. H. (1993) Connexin mutations in X-linked Charcot-Marie-Tooth disease. *Science* **262,** 2039–2042.
16. Fairweather, N., Bell, C., Cochrane, S., Chelly, J., Wang, S., Mostacciuolo, M. L., Monaco, A. P., and Haites, N. E. (1994) Mutations in the connexin32 gene in X-linked dominant Charcot-Marie-Tooth disease (CMTX1). *Hum. Mol. Genet.* **3,** 29–34.
17. Kelsell, D. P., Dunlop, J., Stevens, H. P., Lench, N. J., Liang, J. N., Parry, G., Mueller, R. F., and Leigh, I. M. (1997) Connexin26 mutations in hereditary non-syndromic sensorineuronal deafness. *Nature* **387,** 80–83.
18. Mackay, D., Ionides, A., Berry, V., Moore, A., Bhattacharya, S., and Shiels, A. (1997) A new locus for dominant "zonular pulverulent" cataract on chromosome 1q. *Am. J. Hum. Genet.* **60,** 1474–1478.
19. Shiels, A., Mackay, D., Ionides, A., Berry, V., Moore, A., and Bhattacharya, S. (1997) A missense mutation in the human connexin50 gene (GJA 8) underlies autosomal dominant "zonular pulverulent" cataract, on chromosome 1 q. *Am. J. Hum. Genet.* **62,** 526–532.
20. Richard, G., Smith, L. E., Bailey, R. A., Itin, P., Hohl, D., Epstein, E. H., Jr., DiGiovanna, J. J., Compton, J. G., and Bale, S. J. (1998) Mutations in the human connexin gene GJB3 cause erythrokeratodermia variabilis. *Nat. Genet.* **20,** 366–369.
21. Oh, S., Ri, Y., Bennett, M. V. L., Trexler, E. B., Verselis, V. K., and Bargiello, T. A. (1997) Changes in permeability caused by connexin32 mutations underlie Charcot-Marie-Tooth disease. *Neuron* **19,** 927–938.
22. Cochrane, S., Bergoffen, J., Fairweather, N. D., Muller, E., Mostacciuolo, M. L., Monaco, A. P., Fischbeck, K. H., and Haites, N. E. (1994) X-linked Charcot-Marie-Tooth disease (CMTX1)—A study of 15 families with 12 highly informative polymorphisms. *J. Med. Genet.* **31,** 193–196.
23. Krutovskikh, V., Mironov, N., and Yamasaki, H. (1996) Human connexin 37 is polymorphic but not mutated in tumours. *Carcinogenesis* **17,** 1761–1763.
24. Sato, K., Gratas, C., Lampe, J., Biernat, W., Kleihues, P., Yamasaki, H., and Ohgaki, H. (1997) Reduced expression of P2 form of the gap junction protein connexin43 in malignant meningiomas. *J. Neuropathol. Exp. Neurol.* **7,** 835–839.
25. Reed, K. E., Westphale, E. M., Larson, D. M., Wang, H. Z., Veenstra, R. D., and Beyer, E. C. (1993) Molecular cloning and functional expression of human connexin37, an endothelial cell gap junction protein. *J. Clin. Invest.* **91,** 997–1004.
26. Veenstra, R. D., Wang, H. Z., Beyer, E. C., Ramanan, S. V., and Brink, P. R. (1994) Connexin37 forms high conductance gap junction channels with subconductance state activity and selective dye and ionic permeabilities. *Biophys. J.* **66,** 1915–1928.
27. Boerma, M., Forsberg, L., Van Zeijl, L., Morgenstern, R., DeFaire, U., Lemne, C., Erlinge, D., Thulin, T., Hong, Y., and Cotgreave, I. A. (1999) A genetic polymorphism in connexin 37 as a prognostic marker for atherosclerotic plaque development. *J. Intern. Med.* **246,** 211–218.
28. Varadaraj, K., and Skinner, D. M. (1994) Denaturants or cosolvents improve the specificity of PCR amplification of a G + C-rich DNA using genetically engineered DNA polymerases. *Gene* **140,** 1–5.
29. Kozak, M. (1987) An analysis of 5′-noncoding sequences from 699 vertebrate messenger RNAs. *Nucleic Acid Res.* **15,** 8125–8148.
30. Varadaraj, K., Kumari, S. S., and Skinner, D. M. (1996) Actin-encoding cDNAs and gene expression during the intermolt cycle of the Bermuda land crab *Gecarcinus lateralis*. *Gene* **171,** 177–184.
31. Laemmli, U. K. (1970) Cleavage of structural proteins during the assembly of the head of the bacteriophage T4. *Nature* **227,** 680–685.
32. Kumari, S. S., and Skinner, D. M. (1993) Proteins of crustacean exoskeleton II: immunological evidence for their relatedness to cuticular proteins of two insects. *J. Exp. Zool.* **265,** 195–210.
33. Varadaraj, K., Kushmerick, C., Baldo, G. J., Bassnett, S., Shiels, A., and Mathias, R. T. (1999) The role of MIP in lens fiber cell membrane transport. *J. Membr. Biol.* **170,** 191–203.
34. Veenstra, R., and Brink, P. R. (1992) Patch clamp methods applied to gap channels. *In* Cell-Cell Interactions: A Practical Approach. (Stevenson, B. R., Gallin, W. J., and Paul, D. L., Eds.), IRL Press at Oxford University Press.
35. Brink, P. R., Cronin, K., Banach, K., Peterson, E., Westphale, E. M., Seul, K. H., Ramanan, S. V., and Beyer, E. C. (1997) Evidence for heteromeric gap junction channels formed from rat connexin43 and human connexin37. *Am. J. Physiol. (Cell Physiol.)* **42,** C1386–C1396.
36. Valiunas, V., Bukauskas, F. F., and Weingart, R. (1997) Conductances and selective permeability of connexin43 gap junction channels examined in neonatal rat heart cells. *Circ. Res.* **80,** 708–719.
37. Ramanan, S. V., Brink, P. R., Varadaraj, K., Peterson, E., Schirrmacher, K., and Banach, K. (1999) A three-state model for connexin37 gating kinetics. *Biophys. J.* **76,** 2520–2529.
38. Banach, K., Ramanan, S. V., and Brink, P. R. (2000) The high conductance of human connexin37 is determined by surface charges on the protein. *Biophys. J.* **78,** 952–960.
39. Rubin, J. B., Verselis, V. K., Bennett, M. V. L., and Bargiello, T. A. (1992a) A domain substitution procedure and its use to analyze voltage dependence of homotypic gap junctions formed by connexins 26 and 32. *Proc. Natl. Acad. Sci. USA* **89,** 3820–3824.
40. Rubin, J. B., Verselis, V. K., Bennett, M. V. L., and Bargiello, T. A. (1992b) Molecular analysis of voltage dependence of heterotypic gap junctions formed by connexin 26 and 32. *Biophys. J.* **62,** 183–195.
41. Elenes, S., Chanson, M., and Moreno, A. P. (2000) The carboxyl-terminal of connexin43 modulates channels' unitary conductance distribution and their voltage gating. *Biophys. J.* **78,** 1887a. (Abstr.).
42. Lau, A. F., Kurata, W. E., Kanemitsu, M. Y., Loo, L. W., Warn-Cramer, B. J., Eckhart, W., and Lampe, P. D. (1996) Regulation of connexin43 function by activated tyrosine protein kinases. *J. Bioener. Biomemb.* **28,** 359–368.
43. Warn-Cramer, B. J., Lampe, P. D., Kurata, W. E., Kanemitsu, M. Y., Loo, L. W., Eckhart, W., and Lau, A. F. (1996) Characterization of the mitogen-activated protein kinase phosphorylation sites on the connexin-43 gap junction protein. *J. Biol. Chem.* **271,** 3779–3786.